

EFFECT OF BORON DOPING ON HIGH RESOLUTION X-RAY DIFFRACTION METROLOGY****M. Faheem^{*}, Y. Zhang, X. Dai**

GLOBALFOUNDRIES Inc., 400 Stone Break Extensions, Malta, NY 12020;

e-mail: faheem2001@gmail.com

The effect of boron (B) doping on high-resolution X-ray diffraction (HXRД) metrology has been investigated. Twelve samples of $\text{Si}_{1-x}\text{Ge}_x$ films were epitaxially grown on Si (100) substrates with different thicknesses, germanium (Ge) concentrations and with/without B dopants. Secondary ion mass spectroscopy (SIMS) and HXRД were employed for measurements of B doping, Ge concentration, strain, and thickness of the layers. The SIMS results show the absence of B in two samples while the rest of the samples have B doping in the range of 8.40×10^{18} – 8.7×10^{20} atoms/cm³ with Ge concentration of 13.3–55.2 at.%. The HXRД measurements indicate the layers thickness of 7.07–108.13 nm along with Ge concentration of 12.82–49.09 at.%. The difference in the Ge concentration measured by SIMS and HXRД was found to depend on B doping. For the undoped samples, the difference is ~0.5 at.% and increases with B doping but with no linear proportionality. The difference in the Ge concentration was 7.11 at.% for the highly B doped (8.7×10^{20} atoms/cm³) sample. The B doping influences the $\text{Si}_{1-x}\text{Ge}_x$ structure, causing a change in the lattice parameter and producing tensile strains shifting $\text{Si}_{1-x}\text{Ge}_x$ peaks towards Si (100) substrate peaks in the HXRД diffraction patterns. As a result, Vegard's law is no longer effective and makes a high impact on the HXRД measurement. The comparison between symmetric (004) and asymmetric (+113, +224) reciprocal space mappings (RSM) showed a slight difference in Ge concentration between the undoped and lower B doped samples. However, there is a change of 0.21 at.% observed for the highly doped $\text{Si}_{1-x}\text{Ge}_x$ samples. RSM's (+113) demonstrate the small SiGe peak broadening as B doping increases, which indicates a minor crystal distortion.

Keywords: thin films, SiGe, boron doping, high-resolution X-ray diffraction, secondary ion mass spectroscopy.

ВЛИЯНИЕ ЛЕГИРОВАНИЯ БОРОМ НА МЕТРОЛОГИЮ ВЫСОКОРАЗРЕШАЮЩЕЙ РЕНТГЕНОВСКОЙ ДИФРАКЦИИ**M. Faheem^{*}, Y. Zhang, X. Dai**

УДК 539.216.2

GLOBALFOUNDRIES Inc., 400 Стоун Брейк Экстеншинз, Мальта, штат Нью-Йорк 12020;

e-mail: faheem2001@gmail.com

(Поступила 17 ноября 2016)

Исследовано влияние легирования бором (B) на результаты измерений с помощью высокоразрешающей рентгеновской дифракции (HXRД). 12 образцов пленок $\text{Si}_{1-x}\text{Ge}_x$ эпитаксиально выращены на кремниевых Si (100) подложках разной толщины с различной концентрацией германия (Ge) при наличии и без добавок бора. Для измерения концентрации добавки B, содержания Ge, деформации и толщины слоев использованы методы масс-спектропии вторичных ионов (SIMS) и HXRД. Результаты SIMS свидетельствуют об отсутствии B в двух образцах. В остальных образцах концентрация бора $[B] = 8.40 \times 10^{18}$ – 8.7×10^{20} атомов/см³ при содержании $[Ge] = 13.3$ – 55.2 ат.%. Согласно HXRД-

** Full text is published in JAS V. 85, No. 1 (<http://springer.com/10812>) and in electronic version of ZhPS V. 85, No. 1 (http://www.elibrary.ru/title_about.asp?id=7318; sales@elibrary.ru).

измерениям, толщина слоев составляет 7.07–108.13 нм при $[Ge] = 12.82–49.09$ ат.%. Разница в концентрации Ge, измеренной методами SIMS и HXRD, зависит от легирования бором. Для беспримесных образцов различие составляет ~0.5 ат.% и увеличивается с добавкой B, но не линейно. Для сильнолегированного бором (8.7×10^{20} атомов/см³) образца разница в концентрации Ge 7.11 ат.%. Легирование бором влияет на структуру $Si_{1-x}Ge_x$, вызывая изменения постоянной решетки, и создает деформации растяжения, сдвигая пики $Si_{1-x}Ge_x$ к пикам подложки Si (100) в дифрактограммах HXRD. В результате правило Вегарда не действует, и это сильно влияет на измерения методом HXRD. Сравнение симметричных (004) и асимметричных (+113, +224) обратных пространственных отображений (RSM) показывает небольшое различие концентрации Ge в нелегированных и слаболегированных образцах. Однако для сильнолегированных образцов $Si_{1-x}Ge_x$ изменение достигает 0.21 ат.%. В данных по RSM (+113) наблюдается небольшое уширение пика SiGe при увеличении содержания примеси B, что свидетельствует о незначительной деформации кристалла.

Ключевые слова: тонкая пленка, SiGe, легирование бором, высокоразрешающая рентгеновская дифракция, масс-спектропия вторичных ионов.

Introduction. Due to low cost, good thermal conductivity, and widespread availability, silicon (Si) substrates are widely used in semiconductor industry. Several heterostructures on Si substrates with different lattice constant have been grown for different electronics and optoelectronics applications [1–4]. Among them, silicon germanium (SiGe) gave rise to great interest because of its several technological applications such as optoelectronics [5], modulation-doped field effect transistors (MODFETs) [6], metal oxide field effect transistors (MOSFETs) [7], thin film transistors (TFTs) [8], and heterojunction bipolar transistors (HBTs) [9]. These devices require thin SiGe films with low crystal defects, smooth surface, and high interfacial adhesion strength. Ion implantation and dopant activation in SiGe layers are crucial. The dopants enhance mobility of electrons and holes. The doping level may be subject to change independently of the Ge fraction. As a result, the measurement becomes more complex because of the effect that the dopants make on the structure of the SiGe layers [10]. Change in the dopant level can introduce significant errors to the measurements of Ge concentration. Thus, the large lattice mismatch (~4%) between silicon and germanium along with doping can lead to high-density crystal defects. Such defects can cause metrology issues that ultimately affect the device performance.

There is a high demand for a nondestructive, absolute, calibration-free, and accurate characterization method that controls the Ge content. To date, several methods have been used to investigate the Ge concentration, such as secondary mass ion spectroscopy (SIMS) [11], auger electron spectroscopy (AES) [12], Rutherford backscattering spectrometry (RBS) [13], and high resolution X-ray diffraction (HXRD) [14]. However, SIMS and AES are destructive techniques and cannot provide strain information. In addition, these techniques require vacuum compatible samples and need references for accurate measurements. RBS requires larger surface area (~2 mm) samples. On the other hand, HXRD is a fast and nondestructive technique that requires no sample preparation. It is extremely helpful for epitaxial film characterization and can provide information such as lattice mismatch, substrate orientation, tilt, mosaic spread, wafer curvature, layer thickness, concentration, and inhomogeneity. Among them, layer thickness, concentration, and strain/relaxation information are of specific interest. However, the HXRD technique is limited to a certain level of concentration, which complicates dopant measurements and requires a crystalline surface for analysis. Furthermore, dopant concentrations distort the layer unit volume cell, which affects the HXRD measurements.

In this paper, the effect of boron (B) doping on HXRD metrology has been studied. The SiGe layers with different thicknesses and concentrations were epitaxially grown on Si (100) substrates. Two types of samples were prepared, undoped and B doped. This paper has two aims: to demonstrate the boron doping effect on Ge concentration by comparison SIMS and HXRD measurements, and to compare Ge concentration measured by HXRD symmetric (004) and asymmetric (+113 and +224) scans.

Experiment. For this work, 12 samples of epitaxial SiGe layers on Si (100) substrates were deposited on 12-inch wafers in a commercially available low-pressure chemical vapor deposition system. SiH₄ and DCS (SiCl₂H₂ – dichlorosilane) were used as the source gases for Si, and GeH₄ was used as the source gas for Ge. An appropriate amount of HCL gas was used to maintain the selectivity of the process. Boron was co-deposited with SiGe using B₂H₆ precursor. Among the 12 samples, two samples have undoped SiGe films and the rest of the SiGe samples have B doping in the range of 10^{18} to 10^{20} atoms/cm³. All samples were prepared under the same processing condition.

A Cameca SIMS-MS was used to determine B doping and Ge concentration. SIMS profiles were obtained with impact energy of 500 eV using an O_2^+ source. Electron flooding was employed for charging compensation. The HXRD characterization was performed using a Bruker D8 Fabline for rocking curves and reciprocal space mapping (RMS). The $CuK_{\alpha 1}$ source with a step size of 0.005° and scan time of 10 s was used to measure diffraction patterns. Germanium concentrations were measured using symmetric scans (004 rocking curves) and asymmetric (RSM of +113 and +224) scans.

Results and discussion. All SiGe samples deposited on the Si (100) substrates have different thicknesses and concentrations. In these layers, estimation of B doping and Ge concentration is essential. Due to the size of dopant atoms compared to the host atoms, a structural change in the doped layers can be observed. Figure 1a demonstrates the B doping in the first six samples, where it is estimated to range from 0 – 9.40×10^{19} atoms/cm³. As shown in the Fig. 1, samples 1 and 2 are undoped. The other four samples have doping in the range of 8.40×10^{18} – 9.40×10^{19} atoms/cm³. Higher B doped samples are presented in Fig. 1b. These samples have different thicknesses with B doping on the order of 10^{20} atoms/cm³. The overall B doping is in the range of 0 – 8.70×10^{20} atoms/cm³.

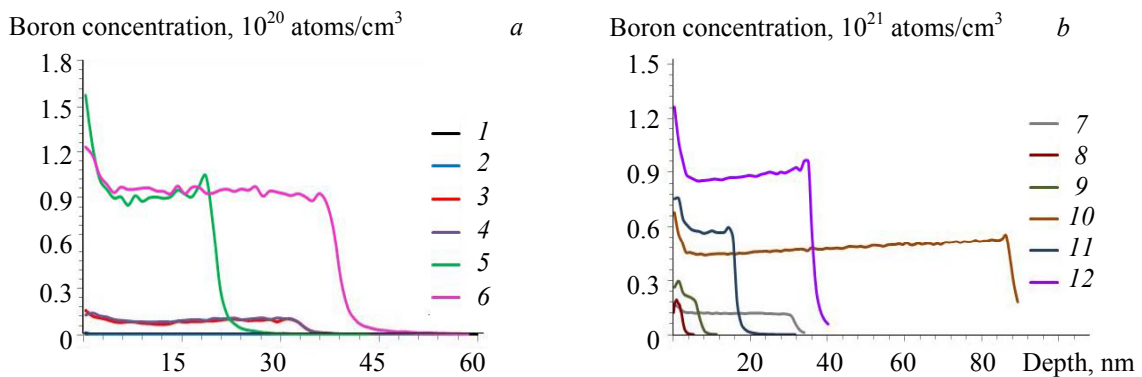


Fig. 1. Boron concentrations determined by SIMS for all samples.

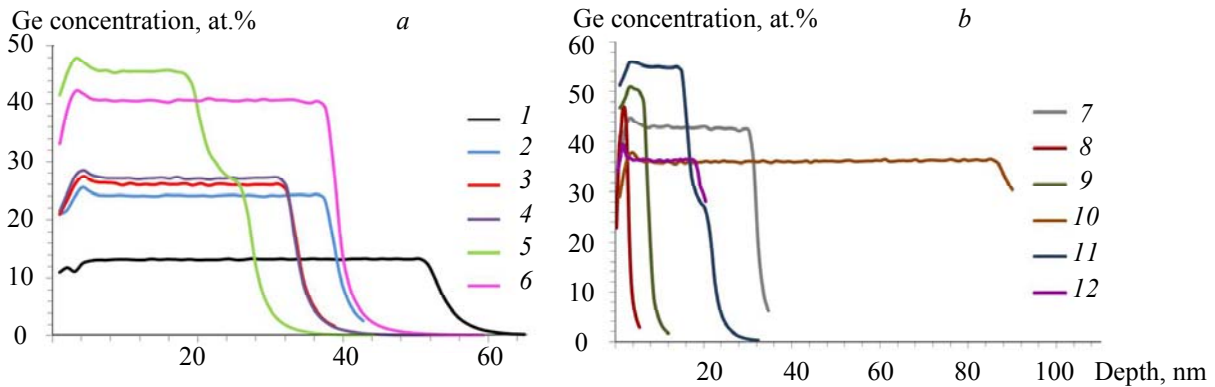


Fig. 2. Germanium concentrations measured by SIMS.

Another important parameter is the Ge concentration as determined by SIMS. Figure 2a shows the Ge concentration of the first six samples with low B doping. The Ge concentrations range from 13.3–40.7 at.%. From Fig. 3b, the Ge concentration is observed in the range of 31.5–48.63 at.%. It is clear from Fig. 2 that all samples possess different Ge concentrations and layer thicknesses.

Two modes of HXRD are employed in this study to understand SiGe behavior: (i) $\omega/2\theta$ scan (rocking curves), which is a fast method from which Ge content and layer thickness of the heterostructure can be measured, and (ii) RMS, a method that is used to determine strain/relaxation and defects. The $\omega/2\theta$ scan is a one-dimensional measurement. In this case, different planar spacings in a certain crystal orientation are probed. Usually, it is the (004) reflection that is measured because it provides high intensity. For a SiGe/Si sample, the reciprocal lattice points corresponding to the silicon substrate and the SiGe layer are observed as

two peaks, as shown in Fig. 3. Symmetric scans (004) corresponding to the first six samples are shown in Fig. 3a. The rocking curves (004) present well-defined thickness fringes, and Ge concentration can be extracted from peak positions. The same behavior of the SiGe layers is observed for the rest of the six samples as shown in Fig. 3b. Oscillations around the peaks are also related to the thickness of the layer. The oscillations are known for finite thickness fringes, and they are caused by X-ray reflections at the layer interfaces. They only occur in a perfect structure with no/less interfacial defects because of coherent diffraction [15] across the interface. In other words, the oscillation characteristics indicate high epitaxial growth of all our SiGe layers deposited on the Si substrates.

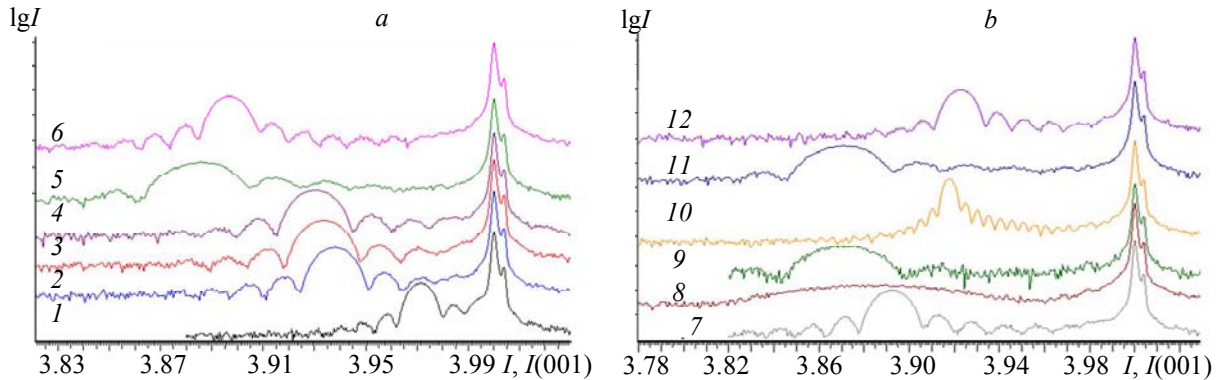


Fig. 3. HXRD measurements of all 12 samples.

The angular separation with respect to the substrate position is directly related to the Ge concentration of the $\text{Si}_x\text{Ge}_{1-x}$ layers. The increase in the distance between Si substrate and SiGe peaks means higher concentration and vice versa. Starting from a model based on the nominal sample structure, the thickness and Ge content of the SiGe layers were refined until a close match between the experimental and simulated curves was obtained by means of automatic fitting using the Bruker software “Leptos”. The Ge content in the SiGe layer can be determined with Vegard’s law. This method is based on some assumptions that must be fulfilled; there must be a perfect fit between the substrate and layer (i.e., no mismatch or partly relaxation), and the layer must be elastically distorted. The improved form of Vegard’s law for thin SiGe layer is used in Leptos [16]

$$\text{Si}_{1-x}\text{Ge}_x = 0.5431 + 0.01992x + 0.00272x^2,$$

where 0.5431 nm is the Si lattice constant and x is the Ge contents. In Fig. 3, samples have random Ge concentrations depending upon the angular separation between SiGe and Si substrate peaks. The corresponding numerical results are summarized in Table 1.

TABLE 1. Layer Thickness, Ge Concentration, and B Doping Determined by SIMS and HXRD

Sample	XRD-thickness, nm	XRD-Ge, at.%	SIMS-Ge, at.%	SIMS-B, atoms/cm ³
1	52.41	12.82	13.3	0
2	40.02	23.7	24.2	0
3	36.28	25.39	26	8.40×10^{18}
4	35.93	26.58	27.2	9.50×10^{18}
5	26.41	44.5	45.6	9.10×10^{19}
6	46.52	39.09	40.7	9.40×10^{19}
7	38.02	40.63	42.7	1.20×10^{20}
8	7.07	43.9	46.4	1.80×10^{20}
9	18.22	47.23	50.6	2.10×10^{20}
10	108.13	31.55	36.2	4.80×10^{20}
11	24.31	49.09	55	5.70×10^{20}
12	47.52	29.39	36.5	8.70×10^{20}

Table 1 displays the B doping/Ge concentration determined by SIMS and thickness/Ge concentration measured by HXRD. As shown in the Table 1, B doping and thickness were only determined by SIMS and HXRD respectively, while Ge contents were measured by both techniques. The SiGe layer thickness varies from 7.07 to 108 nm and B doping from 0– 8.7×10^{20} atoms/cm³. The comparison between Ge concentrations showed the difference. The difference in Ge concentrations corresponding to B doping is presented in Fig. 4. For the undoped B samples, the difference in Ge concentrations is less than 0.5 at.%. This small difference can be due to the nature of two different techniques. For the 10^{18} atoms/cm³ B doping range, there is a slight change observed in Ge concentration. As B doping increases, the SiGe peak starts moving towards the substrate peak in the HXRD diffraction pattern. The distance between SiGe and substrate peaks is proportional to Ge concentration. The difference in Ge concentration increases as B doping increases in the range of 10^{19} atoms/cm³. However, there is a huge difference in Ge concentration observed in the range of 1.20 – 8.70×10^{20} atoms/cm³.

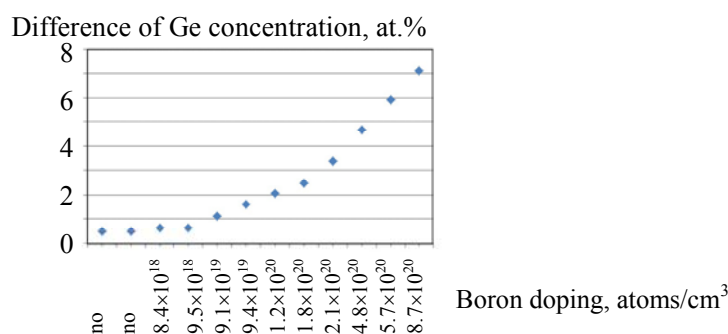


Fig. 4. Difference in Ge concentration measured by SIMS and HXRD versus B doping.

It can be seen that the difference of Ge concentration in the doped SiGe layers with respect to each other apparently depends upon the B doping level. Previously, B diffusion in SiGe was studied extensively [10, 17–20]. $\text{Si}_{1-x}\text{Ge}_x$ has the same lattice structure as Si but with a larger lattice constant. Boron diffusion is found to decrease with increasing Ge content [19]. In addition, B diffusion decreased in SiGe/Si heterostructures when strain increased in the SiGe layer due to the lattice mismatch [20]. Our results agreed with the previous work, however, the relation between differences in the B doping and Ge concentrations is not linear. There are two parameters that play an important role: (i) Ge concentration that increases the lattice constant of SiGe, (ii) B doping that contracts the unit volume cell and lowers the lattice contact. From the Table 1, it can be seen that Ge concentration is in the range of 36.2 to 55 at.% and is randomly deposited for 10^{20} atoms/cm³ B doping. Hence, the key driving force responsible for the Ge concentration difference is the B doping.

In order to understand the B doping effect on different reflections, asymmetrical reciprocal space maps (RSM) were constructed on three samples: (i) sample 1, which is undoped (ii), sample 6 with the B doping of 9.40×10^{19} atoms/cm³, and (iii) highly B doped sample 12. The silicon lattice is not a simple cubic lattice but a face-centered cubic (*fcc*) lattice with a two atom bases. The reciprocal lattice of the *fcc* lattice is a body-centered cubic (*bcc*) lattice, of which the cubic lattice is a subset, and due to the two-point bases, a geometrical structure factor will cause the intensity of the reflections to vary. In Fig 5, the reciprocal lattice of Si/SiGe for asymmetrical scans (+113) and (+224) is shown. Since the SiGe layers are strained and have the same lattice parameter as the substrate, a reciprocal lattice point of the strained layer will appear directly below the lattice point of the substrate, as shown in Fig. 5.

The Ge concentration repeatability for (004) scans was studied using undoped sample 1 in the dynamic and static modes. In each case, 10 measurements were carried out. For all measurements, the difference in Ge concentration was lower than 0.1 at.%. Next, all asymmetrical scans were integrated into one-dimensional scans to determine Ge concentrations. The Ge concentrations measured from (+113) and (+224) RSM scans were compared with the symmetric scan (004). For the undoped sample, the difference in Ge concentration was ~0.06 at.% and for sample 6, the difference was less than 0.08 at. %. These differences are under repeatability tolerance of 0.1 at.%. For the highly doped sample, the difference in Ge concentration was 0.12 and 0.21 at.% for (+113) and (+224) scans, respectively. Therefore, a slight change in Ge concentration was

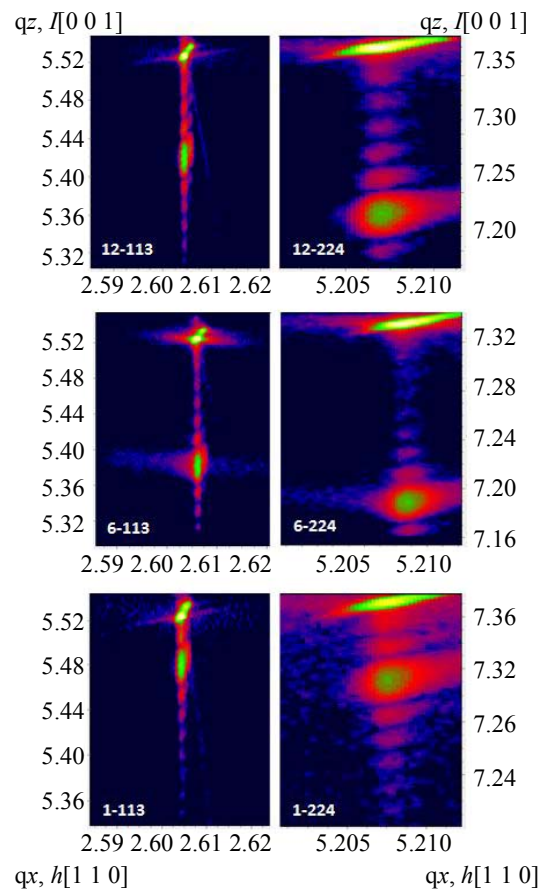


Fig. 5. Asymmetric scans (+113 and +224) of samples 1, 6, and 12.

observed for the highly B doped sample. All asymmetric scans showed that the SiGe layers are strained. The SiGe peaks for samples 6 and 12 present more broadening in the transverse direction. The broadening in the SiGe peaks is caused by dislocations that distort the lattice planes. Hence, higher B doping affects the lattice structure.

Conclusion. A series of $\text{Si}_{1-x}\text{Ge}_x$ samples was prepared with different thickness and Ge concentration to study the B doping effect. The B doping was found within the range of $0\text{--}8.70 \times 10^{20}$ atoms/cm³. SIMS was employed to determine the B doping and Ge concentration. HXRD was used to measure thickness and Ge concentration. There is a slight difference observed in Ge concentration measured by the two techniques for the undoped samples. The difference in Ge concentration increases as the B doping increases. However, the difference is much higher ($\sim 2.07\text{--}7.11$ at.%) in the range of $(1.20\text{--}8.70) \times 10^{20}$ atoms/cm³. Such difference in Ge concentrations (5.04 at.%) for a short range of the B doping (10^{20} atoms/cm³) leads to a discrepancy of Vegard's law and makes the HXRD measurements unreliable. A series of equations (Vegard's law) corresponding to B concentration can be established based on the B doping to overcome this problem. The results also demonstrate that there is no linear relationship between the B doping and the difference in Ge concentrations. A comparison of symmetric and asymmetric (+113, +224) scans showed the difference of 0.12 and 0.21 at.% for the highly B doped samples. All SiGe layers are strained with a minor lattice distortion for the higher B doped samples.

Acknowledgment. The authors would like to thank Dr. Zeynel Bryinder for useful discussions.

REFERENCES

1. Qing Hua Wang, Kourosh Kalantar-Zadeh, A. Kis, J. N. Coleman, M. S. Strano, *Nature Nanotechnol.*, **7**, 702–712 (2012).
2. F. Bonaccorso, Z. Sun, T. Hasan, A. C. Ferrari, *Nature Photonics*, **4**, 611–622 (2010).

3. M. Z. Mohd Yusoff, A. Mahyuddin, Z. Hassan, Y. Yusof, M. A. Ahmad, C. W. Chin, H. Abu Hassan, M. J. Abdullah, *Superlattices Microstruct.*, **60**, 500–550 (2013).
4. Wai Hoe Tham, Ding Shenp Ang, Lakshmi Kanta Bera, Surani Bin Dolmanan, Thirumaleshwara N. Bhat, Vivian K. X. Lin, Sudhiranjan Tripathy, *IEEE Trans. Electron. Devices*, **63**, No. 1, 345–351 (2016).
5. X. Chen, K. Liu, Q. C. Quyang, S. K. Jayanarayanan, S. K. Banerjee, *IEEE Trans. Electron. Devices*, **48**, 1975–1980 (2001).
6. Kamal Prakash Pandey, Rakesh Kumar Singh, Anil Kumar, *Int. J. Adv. Res. Comput. Commun. Eng.*, **2**, No. 4, 1831–1834 (2013).
7. A. K. Okyay, A. J. Pethe, D. Kuzum, S. Latif, D. A. B. Miller, Kr. C. Saraswat, *Opt. Lett.*, **32**, No. 14, 2022–2024 (2007).
8. M. Mitsui, K. Arimoto, J. Yamanaka, K. Nakagawa, K. Sawano, Y. Shiraki, *Appl. Phys. Lett.*, **89**, 192102-05 (2006).
9. J.-S. Rieh, B. Jagannathan, D. R. Greenberg, M. Meghelli, A. Rylyakov, F. Guarin, Zh. Yang, D. C. Ahlgren, G. Freeman, P. Cottrell, D. Hareme, *IEEE Trans. Microwave Theory Techn.*, **52**, No. 10, 2390–2407 (2004).
10. J. F. Woitok, C. C. G. Visser, T. L. M. Scholtes, *Mater. Sci. Eng.*, **B89**, 216–220 (2002).
11. H. Rucker, B. Heinemann, *Solid State Electron.*, **44**, 783–789 (2000).
12. M. Valden, S. Pak, X. Lai, D. W. Goodman, *Catal. Lett.*, **56**, 7–10 (1998).
13. N. Sugiyama, T. Mizuno, S. Takagi, M. Koike, A. Kurobe, *Thin Solid Films*, **369**, No. 3, 199–202 (2000).
14. M. Faheem, A. Kumar, Y. Liang, P. van Der Heide, *Mater. Sci. Semiconductor Proc.*, **44**, No. 15, 8–12 (2016).
15. P. F. Fewster, *J. Appl. Crystallogr.*, **25**, 714–723 (1992).
16. DIFFRAC Plus, Bruker's User Manual, DOC-M88-EXX052, **7**, No. 2–5 (2009).
17. Yong Seok Suh, M. S. Carroll, R. A. Levy, G. Bisognin, D. de Salvador, M. A. Sahiner, C. A. King, *IEEE Trans. Electron. Devices*, **52**, No. 11, 2416–2421 (2005).
18. Y. Bogumilowicz, J. M. Hartmann, *Thin Solid Films*, **557**, 4–9 (2014).
19. N. R. Zangenberg, J. Fage-Pedersen, J. Lundsgaard Hansen, A. Nylandsted Larsen, *J. Appl. Phys.*, **94**, 3883–3889 (2003).
20. N. E. B. Cowern, P. C. Zalm, P. van der Sluis, D. J. Gravesteijn, W. B. de Boer, *Phys. Rev. Lett.*, **72**, 2585–2588 (1994).